Journal Name

COMMUNICATION

Superior cycle and rate performance of a novel sulfur cathode by immobilizing sulfur into porous N-doped carbon microspheres

Hui Xu,[b] Yuanfu Deng,*[a,b] Zhenxia Zhao,[a,b] Hongjie Xu,[c] Xusong Qin[b] and Guohua Chen*[b,c]

A novel composite of sulfur immobilized into porous N-doped carbon microspheres (NCMSs/S) was synthesized. The composite cathode for Lithium-sulfur batteries delivers a high specific capacity and superior rate capability and cycle stability, with a reversible capacity of ~ 605mAh g^{-1} at 2 C and 85% capacity retention after 500 cycles.

Lithium-sulfur (Li-S) batteries have received increasing attention due to their low-cost, high theoretical energy (2567 Wh kg^{-1}) and environmental friendliness.[1] However, their wide industrial applications have been hindered by the problems related to the sulfur cathode as low conductivity of the sulfur,[2] loss of active materials and the redox shuttle induced by lithium polysulfide dissolution in the electrolyte.[3] To meet these challenges, the most frequently adopted strategy is to incorporate Sinto carbon matrix such as mesoporous carbon,[4] microporous carbon,[5] carbon nanotube (CNT),[6] porous hollow carbon spheres,[7] porous carbon fibers,[8] graphene/graphene oxides[9] and nitrogen-doped mesoporous carbon.[10] Based on this point, high specific capacities exceeding 1000 mAh g^{-1} under 0.1 C [4a,5b,7d,8b,9b,10] and good rate performance (> 600 mAh g^{-1} at 2.0 C) have been achieved in the recently literatures.[6c,6d,9h]

The ideal configuration for a S/carbon cathode is to have high conductivity of the carbon matrix, homogenous S dispersion, complete sulfur encapsulation in a confined but accessible space with strong sulfur-matrix affinity to obtain high specific capacity (full sulphur utilization), excellent capacity retention and good rate performance.[11] Most of the previous results are only of one or two characteristics listed above. For example, S encapsulated into micro-porous carbon materials would show good cycling performance.[5a] Lithiation potential hysteresis, however, may occur during the discharge/charge process due to the high diffusion resistance in micro-porous carbon matrix.[5a] The graphene oxide-S nano-composites deliver high specific capacity and outstanding cyclability at 0.1 C rate. However, an ordinary rate performance was obtained.[9b] Despite substantial progress has been made, there are strong demand for the cathode materials with long-cycle stability at high rate for industrial Li-S batteries.[12]

In this work, we report a rational design and synthesis of a novel N-doped carbon/sulfur (NCMSs/S) composite by confining sulfur in porous NCMSs. Such porous NCMSs with micro- and meso-pores and the method used to infuse S into the pores are designed with four specific aims in mind: 1) enhancement of the conductivity of the porous NCMSs for facilitating good transport of electrons from the poorly conducting sulfur; 2) immobilization of S tightly in the specific micro-pores by the functional groups to keep intimate contact between the conducting matrix and S species; 3) preservation of fast transport of lithium ions in the mesopores to the sequestered S by ensuring good electrolyte penetration; and 4) utilization of the functional groups in the NCMSs through the electron-donating atoms (N and O) to absorb the polysulfide produced during the electrochemical reaction. When employing such composite as the cathode material in Li-S batteries, promising electrochemical performance upon extended cycling for hundreds of cycles at different current densities were found as discussed subsequently.

The uniform porous NCMSs could be clearly seen from the typical scanning electron microscope (SEM) and transmission electron microscope (TEM) images (Fig. 1a and 1b). Although some meso-pores were detected by N_2 adsorption-desorption (Fig. s1), no obvious pores can be found from the HRTEM image. This may be attributed to the meso-pores formed by interconnecting shells in NCMSs.[10] Thefourier transform infrared (FTIR) spectra (Fig. S1) of the obtained porous NCMSs show the characteristic spectrum of such functional groups as N-H, O-H, C-O and C-N.[13] The porous NCMSs have a high Burnauer-Emmett-Teller (BET) specific area of 724.5 m^2 g^{-1} and a total pore volume of 0.505 cm^3 g^{-1} (the volume of the micro-pores is 0.230 cm^3 g^{-1}). The general shape of the isotherm is defined as Type I according to IUPAC (Fig. 2), revealing a micro-porous structure with a small hysteresis loop. The pore size of the porous NCMSs (inset in Fig. s2) has two levels micro-pores (0.6-0.7 and 0.7-2.0 nm) and small meso-pores (2.0-3.0 nm). As the consequence, the high surface area and moderate pore volume in the porous NCMSs are able to accommodate moderate S loading into the porous conductive network and the

functional groups equip the porous NCMSs with an active surface can provide more active sites for chemically immobilizing sulfur /polysulfide.[10,14]

After loading S into the porous NCMSs, the NCMSs/S composite shows a similar morphology compared to the pristine porous NCMSs (as demonstrated by SEM and TEM images, Figs. 1d and 1e) with smoother surface. However, a significant decrease in BET surface area from 724.5 to 8.40 m^2 g^{-1} and a sharp decrease of the pore volume from 0.505 to 0.03 cm^3 g^{-1} were observed for NCMSs and NCMSs/S, indicating the successful migration of sulfur into the pores. The HRTEM image (Fig. 1f) shows no indication of crystalline sulfur in the NCMSs/S composite. The adsorption of S on carbon likely allowed the S to be uniformly distributed within the framework.[7a,9b,10] The elemental mapping of S, carbon and nitrogen (Fig. s3) also clearly revealed the homogenous distribution of S in the porous NCMSs.
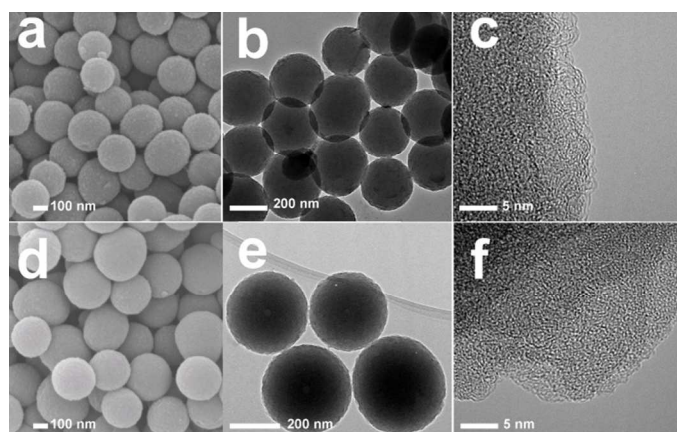
Fig. 1 Images of porous NCMSs and NCMSs/S, (a) the SEM; (b, c) TEM of porous NCMSs; (d) the SEM and (e, f) TEM of NCMSs/S.

The thermogravimeteric analysis (TGA) of the NCMSs/S composite in nitrogen flow shows a total 50% weight loss of S (Fig. s4a). The absence of characteristic peaks for S in the X-ray diffraction pattern indicates a very low degree of crystallization of S in the NCMSs/S composite (Fig. s4b). This suggests that the S is either amorphous or the Snanoparticles trapped/absorbed in the porous NCMSs are unable to crystallize, which is consistent with the HRTEM image. The XRD pattern of the porous NCMSs however has certain degree of crystalline order (two peaks at about 2θ = 25 and 43º), which is indicative of graphitic character for the materials studied here (JCPDS, No. 75-1621). This result was also demonstrated by the Raman and XPS analysis (Fig. s5 and s6). The NCMSs/S composite, with graphitic content of carbon and nitrogen atoms, are attractive because it facilitate transport of electrons from the poorly conductive sulfur,[15] improving the electrochemical stability of the NCMSs/S composite even at high discharge/charge rates. In addition, the peak at $\sim$ 830 cm^{-1} on the Raman spectrum (Fig. s5) suggests that a C-S bond exists in the NCMSs/S composite.[16]

A typical cyclic voltammogram (CV) of the NCMSs/S composite electrode is shown in Fig. s7. No obvious change in the values and locations of the CV peaks were observed upon increasing in the cycle numbers, demonstrating the good electrochemical reversibility of the NCMSs/S composite.[5a] The typical discharge-charge curves of the NCMSs/S composite electrode at rate 0.2 C (1 C = 1672 mA g^{-1}) in the range between 1.5 and 2.8 V are shown in Fig. 2a. The two typical plateaus at 2.3 and 2.1 V in the discharge curve correspond well with the two reduction peaks detected in the CV curves, respectively. The reverse reaction, corresponding to the oxidation of lower-order lithium polysulfides and high-order polysulfides were displayed in the charge curves with a solpe potential from 2.2 to 2.4 V, which corresponds to the main oxidation peak (2.4 V) in the CV curve. The NCMSs/S composite displays an initial specific discharge capacity of 1124 mAh g^{-1} at 0.2 C after activation for a few cycles, and maintains a reversible specific discharge capacity of 1042 mAh g^{-1} after 100 cycles with 92.7% capacity retention (Fig. 2b, inset). The very small capacity loss indicates that the NCMSs/S composite has good capacity retention capability at low rate. It is worth to note that the high discharge capacity and good cyclability of the NCMSs/S compositeare highly reproducible with the other coin cell cycled at 0.5 C rate (Fig. 2b), a specific capacity of 831 mA h g^{-1} wereachieved after 400 cycles with 79% capacity retained. The high specific capacities and good capacity retention capability are comparable to the state-of-the-art S/carbon composites.[4-10]
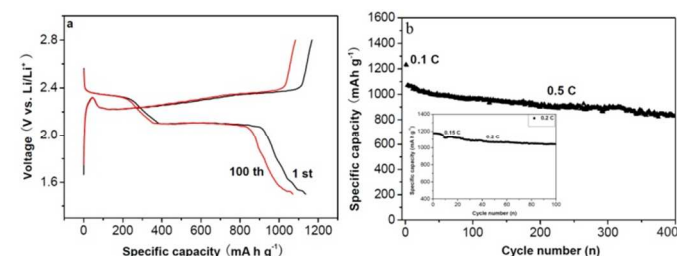
Fig.2 (a) The voltage vs. capacity profiles at 0.2 C rate and (b) the cyclic performance of the NCMSs/S at 0.2 (inset) and 0.5 Crates.
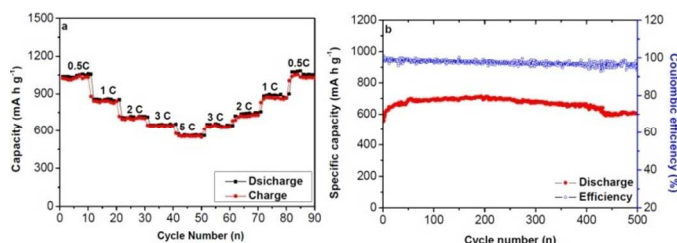
Fig. 3 (a) Rate capability and (b) the cycle life of NCMSs/S composite at 2.0 C rate.

Fig. 3a depicts the rate performance of the NCMSs/S composite. Stable capacities of around 1040, 840, 700, 640 and 560 mA h g^{-1} were obtained at the rates of 0.5, 1.0, 2.0, 3.0 and 5.0 C, respectively. The corresponding discharge/charge curves were displayed in Fig. s8. A capacity of 560 mA h g^{-1} at 5.0 C rate is an impressive result for Li-S batteries cycled at such high rate. This discharge specific capacity is much higher than those values of recently reported S/carbon composites cathodes.[4-5,6a] Important, recovery capacities of 635, 710, 865 and 1035mAh g^{-1} were obtained when the current density of discharge and charge resumed to the rates of 3.0, 2.0, 1.0 and 0.5 C, respectively. Such results give confidence on the usage of NCMSs/S composite in the preparation of cathode for Li-S batteries especially when capacity and rate performances are concerned. Another coin cell cycled at 2 C also shows the superior rate and cycle capability (Fig. 3b), in which a

discharge capacity of 710 mAh g^{-1} after an activation process was obtained. And a reversible capacity of 605 mAh g^{-1} was retained after 500 cycles, with 85% capacity retention. The Coulombic efficiency of the coin cell maintains above 95.0% in the whole 500 cycles.

The electrochemical performance of the sulfur cathode is influenced by many factors, including conductive matrix, binders, electrolyte and modified lithium andoe.[9h,12a,17] However, the N-doped carbon microspheres as conductive matrix is the key issue for improving the electrochemical performance of the NCMSs/S composite cathode. The high-rate charge/discharge capability, the good cycle stability, and the active-sulfur utilization of the NCMSs/S composite cathode are attributed to multiple, possibly synergistic effects that stem from their structural features and reasonable chemical compositions. In the NCMSs/S composite, a novel micro- to meso-pores structure is formed, where the sulfur is highly dispersed in the porous conductive NCMSs (matrix) with such functional groups as N-H, O-H, C-O and C-N. Apparently, the synergistic combination of the immobilizing sulfur of both novel pores and functional groups[10] is the key issue to confine the electrochemical reaction inside the interior pores of the NCMSs due to strong adsorption and interaction of the electron-donating groups and polysulfides via a coordination bond-like mode, which could effectively alleviate the usually observed redox shuttle of soluble lithium polysulfides. Meanwhile, the good mechanical property of the NCMSs, which is demonstrated by the good morphology of the NCMS/S composite after long cycles (Fig. s9), can provide some free space for alleviating the structural strain and tolerating the volume variation associated with the repeated lithium ions insertion/extraction processes, leading to enhanced cycle performance. Finally, the high electrical conductivity originating from the N-doping and some graphitic characters is essential to improve the electrochemical performance of NCMSs/S composite cathode,[15] especially at high discharge/charge rates. This result was also demonstrated by the low resistance of the coin cell made of the NCMs/S composite and the minor resistance alternation after the long cycles (Fig. 10).

Conclusions

In summary, a novel S-immobilized NCMs composite has been successfully designed and assembled as cathode for Li−S batteries with significantly improved cycle stability and rate performance. Because of the synergistic effects that stem from their structural features and reasonable chemical compositions, the composite demonstrates high specific capacity and superior rate performance and cycle stability. The observed very slow decay at 2.0 C (0.030% per cycle for 500 cycles) represents a significant step forward for Li−S batteries, which exceeds the cycling target set by U.S. DOE (Departmentof Energy) in 2011.[9d, 18] These results would shed light on developing novel N or other elements-doped carbon spheres with suitable porous structures for idea sulfur-hosted matrix.

Acknowledgements

Notes and references

^{a}The Key Laboratory of fuel cell of Guangdong province, School of Chemistry and Chemical Engineering, South China University of Technology, Guangzhou, 510640, China,chyfdeng@scut.edu.cn;
^{b}Centre for Green Products and Processing Technologies, Guangzhou HKUST Fok Ying Tung Research Institute, Guangzhou, 511458, China;
^{c} Department of Chemical and Biomolecular Engineering, The Hong Kong University of Science and Technology, Hong Kong, China, kechengh@ust.hk
† Electronic Supplementary Information (ESI) available: See DOI: 10.1039/b000000x/

1 (a) D. Peramunage and S. Licht, *Science*, 1993, **261**, 1029; (b) X. L. Ji and L. F. Nazar, *J. Mater. Chem.*, 2010, **20**, 9821.

2 R. D. Rauh, K. M. Abraham, G. F. Pearson, J. K. Surprenant and S. B. Brummer, *J. Electrochem. Soc.*, 1979, **126**, 523.

3 J. Shim, K. A. Striebel and E. J. Cairns, *J. Electrochem. Soc.*, 2002, **149**, A1321.

4 (a) X. L. Ji, K. T. Lee and L. F. Nazar, *Nat. Mater.*, 2009, **8**, 500; (b) J. Schuster, G. He, B. Mandlmeier, T. Yim, K. T. Lee, T. Bein and L. F. Nazar, *Angew. Chem. Int. Ed.*, 2012, **51**, 3591. (c) Z. Li, L. X. Yuan, Z. Q. Liu, Y. Xin, Z. L. Zhang and Y. H. Huang, *Nanoscale*, 2014, **6**, 1653. (d) Z. Li, L. X. Yuan, Z. Q. Yi, Y. M. Sun, Y. Liu, Y. Jiang,Y. Shen, Y. Xin, Z. L. Zhang and Y. H. Huang, *Adv. Energy Mater.*, 2014, **4**, 1301473.

5 (a) B. Zhang, X. Qin, G. R. Li and X. P. Gao, *Energy Environ. Sci.*, 2010, **3**, 1531; (b) S. Xin, L. Gu, N. H. Zhao, Y. X. Yin, L. J. Zhou, Y. G. Guo and L. J. Wan, *J. Am. Chem. Soc.*, 2012, **134**, 18150.

6 (a) S. Dorfler, M. Hagen, H. Althues, J. Tubke, S. Kaskel and M. J. Hoffmann, *Chem. Commun.*, 2012, **48**, 4097; (b) J. Guo, Y. Xu and C. Wang, *Nano. Lett.*, 2011, **11**, 4288;(c) S. Moon, Y. H. Jung, W. K. Jung, D. S. Jung, J. W. Choi and D. K. Kim, *Adv. Mater.*, 2013, **25**, 6547;(d) S. Q. Chen, X. D. Huang, H. Liu, B. Sun, W. Yeoh, K. F. Li, J. Q. Zhang and G. X. Wang, *Adv. Energy Mater.*, 2014, 1301761.

7 (a) N. Jayaprakash, J. Shen, S. S. Surya, M. A. Corona and L. A. Archer, *Angew. Chem. Int. Ed.*, 2011, **50**, 5904; (b) C. F. Zhang, H. B. Wu, C. Z. Yuan, Z. D. Guo and X. W. Lou, *Angew. Chem. Int. Ed.*, 2012, **51**, 9592;(c) G. He, S. Evers, X. Liang, M. Cuisinier, A. Garsuch and L. F. Nazar, *ACS Nano.*, 2013, **7**, 10920.

8 (a) G. Zheng, Y. Yang, J. J. Cha, S. S. Hong and Y. Cui, *Nano Lett.*, 2011, **11**, 4462; (b) L. W. Ji, M. M. Rao, S. Aloni, L. Wang, E. J. Cairns and Y. G. Zhang, *Energy Environ. Sci.*, 2011, **4**, 5053.

9 (a) H. L. Wang, Y. Yang, Y. Y. Liang, J. T. Robinson, Y. G. Li, A. Jackson, Y. Cui and H. J. Dai, *Nano. Lett.*, 2011, **11**, 2644; (b) L. W. Ji, M. M. Rao, H. M. Zheng, L. Zhang, Y. C. Li, W. H. Duan, J. H. Guo, E. J. Cairns and Y. G. Zhang, *J. Am. Chem. Soc.*, 2011, **133**, 18522; (c) S. Evers and L. F. Nazar, *Chem. Commun.*, 2012, **48**, 1233; (d) S. T. Lu, Y. W. Cheng, X. H. Wu and J. Liu, *Nano Lett.*, 2013, **13**, 2485; (e) H. Xu, Y. F. Deng, Z. C. Shi, Y. X. Qian, Y.Z. Meng and G. H. Chen, *J. Mater. Chem. A*, 2013, **1**, 15142; (f) M. Q. Zhao, Q. Zhang, J. Q. Huang, G. L. Tian, J. Q. Nie, H. J. Peng and F. Wei, *Nature Commun.*, 2014, **5**, 3410; (g) J. P. Rong, M. Y. Ge, X. Fang and C. Zhou, *Nano Lett.*, 2014,**14**, 473;(h) M. K. Song, Y. G. Zhang and E. J. Cairns, *Nano Lett.*, 2014, **14**, 5891.

10 J. X. Song, T. Xu, M. L. Gordin, P. Y. Zhu, D. P. Lv, Y. B. Jiang, Y. S. Chen, Y. H. Duan and D. H. Wang, *Adv. Func. Mater.*, 2014, **24**, 1243.

11 L. Xiao, Y. Cao, J. Xiao, B. Schwenzer, M. H. Engelhard, L. V. Saraf, Z. Nie, G. J. Exarhos and J. Liu, *Adv. Mater.*, 2012, **24**, 1176.

12 (a) J. Kim, D. J. Lee, H. G. Jung, Y. K. Sun, J. Hassoun and B. Scrosati, *Adv. Funct. Mater.*, 2012, **23**, 1076; (b) Y. X. Yin, S. Xin, Y. G. Guo and L. J. Wan, *Angew. Chem. Int. Ed.*, 2013, **52**, 13186.

13 H. S. Li, L. F. Shen, K. B. Yin, J. Ji, J. Wang, X. Y. Wang and X. G. Zhang, *J. Mater. Chem. A*, 2013, **1**, 7270.

14 (a) J. C. Guo, Z. C. Yang, Y. C. Yu, H. D. Abruńa and L. A. Archer, *J. Am. Chem. Soc*., 2013, **135**, 763; (b) G. Y. Zheng, Q. F. Zhang, J. J. Cha, Y. Yang, W. Y. Li, Z. W. She and Y. Cui, *Nano Lett.*, 2013, **13**, 1265.

15 M. C. Dos Santos and F. Alvarez, *Phys. Rev. B*, 1998, **58**, 13918.

16 (a) X. G. Yu, J. Y. Xie, J. Yang, H. J. Huang, K. Wang and Z. S. Wen, *J. Electroanal. Chem.*, 2004, **573**, 12; (b) T. H. Hwang, D. S. Jung, J. S. Kim, B. G. Kim and J. W. Choi, *Nano Lett.*, 2013, 2013, **13**, 4532.

17 Y. J. Jung and S. Kim, *Electrochem. Commun.*, 2007, **9**, 249.

18 D Howell, Fiscal Year 2011 Annual Progress Report for Energy Storage R&D; *U.S. Department of Energy*: Washington, DC, 2012**.**

ChemComm Accepted Manuscript